Crossover from Metastable to Unstable Facet Growth on Si(111)

R. J. Phaneuf, N. C. Bartelt, and Ellen D. Williams
Department of Physics, University of Maryland, College Park, Maryland 20742

W. Swiech and E. Bauer
Physikalisches Institut, Technische Universität Clausthal, D-3392 Clausthal-Zellerfeld, Germany
(Received 10 February 1993)

Vicinal Si(111) surfaces misoriented towards the [$\bar{2}$11] direction facet reversibly upon cooling through the (1×1) to (7×7) reconstructive phase transition. We have used low-energy electron microscopy to examine the kinetics of this phase separation. Nucleation and growth of facets occur when the surfaces are quenched just below the phase boundary. However, at lower temperatures we find evidence for the existence of a spinodal which divides the faceting kinetics into unstable and metastable regions. The location of the spinodal is consistent with previous measurements of Si(111) step energetics.

PACS numbers: 68.35.Md, 61.16.Bg, 81.60.Cp, 82.65.Dp

As surfaces are becoming better characterized, the importance of surface morphology in determining surface characteristics is becoming increasingly evident [1–6]. A dramatic manifestation of the variability of surface morphology is "faceting" in which a flat surface breaks into a hill-and-valley structure, thus increasing total area. One of the most thoroughly studied of the faceting systems is vicinal Si(111) [2,3]. Here surfaces which consist of a uniform array of steps at high temperature facet into singular (111) regions and step "bunches" at low temperature. The faceting is initiated by a change in the surface structure [from (1×1) to (7×7) periodicity], which occurs in a strongly first-order transition at about 870 °C on singular, unstepped surfaces. This faceting is reversible, and there is a well-defined temperature-orientation phase diagram [2] which determines the temperature dependence of the average spacing between steps in a step bunch. In this paper we discuss our low-energy electron microscopy (LEEM) observations of the kinetics of the faceting of these Si surfaces.

The principal result of this paper is that the analogy of faceting with phase separation extends also to the kinetics. In previous work we have focused on the nucleation and growth of facets near the thermodynamic phase boundary, comparing observations with the predictions of the classical theories of nucleated facet growth by Mullins [7,8]. However, in systems which phase separate there is often a sharp transition between temperature regimes in which regions of a second phase nucleate and grow within the first, and lower temperatures where the system is unstable with respect to spontaneous decomposition everywhere into two phases [9]. The line separating these two kinetic regimes is called the *spinodal*. The existence of a spinodal is particularly important in explaining the decomposition of metal alloys [10]. For example, microscopy studies often show marked changes in the morphology of phase separation as a function of quench conditions [11]. Here we present evidence for the existence of a spinodal for vicinal Si(111).

We emphasize at the outset that we expect our observations and arguments to apply generally. From a thermodynamic perspective, faceting induced by the formation of a surface reconstruction is very similar to faceting induced by *impurity* adsorption. Faceting of systems under adsorption is common [6,12], and thus our observations in principle are important for many different systems.

The LEEM used in these experiments is discussed elsewhere [13,14]. The silicon specimens used in this experiment were cut and polished along orientations slightly away from [111] toward [$\bar{2}$11] [2]. In this paper, we concentrate on results obtained with a 4.0° misoriented surface; however, some results for a 0.8° misoriented surface are also briefly mentioned. Specimen preparation is discussed elsewhere [2,3]. The temperature of the sample could be held constant to within 1 °C for tens of minutes.

To examine the kinetics of the faceting, we rapidly quenched the surface from its high temperature state to a lower temperature. Panels (a)–(c) of Fig. 1 show sequences of images of the surface 1, 3, and 60 s after a quench to 840 °C. The bright regions correspond to (7×7) reconstructed (111) terraces. These images show that at this temperature facet formation occurs by the nucleation and growth of isolated linear (7×7) reconstructed (111) facets. As discussed in detail in Ref. [3] the facets quickly reach a stable width. The surface becomes fully faceted via the nucleation and lateral growth of additional facets.

After waiting for the faceting to complete, we slowly heated the surface until the facets disappeared. This procedure allowed the temperature of the thermodynamic phase boundary to be located accurately: For this 4° sample, we find T_0=857 °C. We note that, as might be anticipated (see the discussion below), nucleation rates near the phase boundary are very small: For example, we were able to hold the temperature at 852 °C for 5 min without observing any nucleation events.

Panels (d)–(f) of Fig. 1 show a sequence of images for a quench only 1 °C below the temperature of panels (a)–(c). The growth mode has clearly changed, with

0031-9007/93/71(14)/2284(4)$06.00
© 1993 The American Physical Society

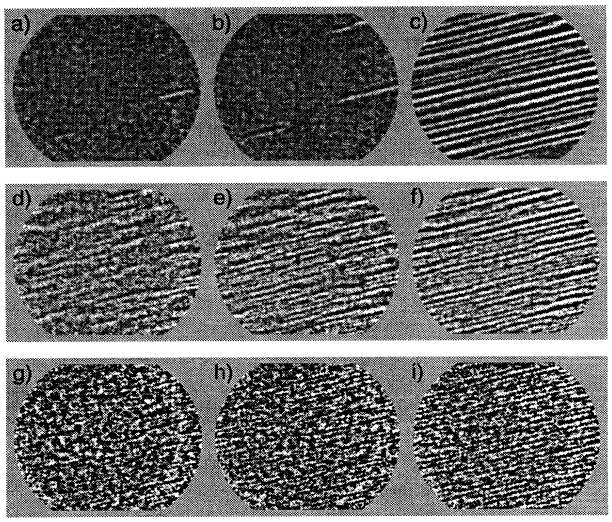

FIG. 1. (a)–(c) A sequence of LEEM images of vicinal Si quenched to 848.3 °C showing nucleation and growth. Initially the surface contains a uniform array of steps which are separated by a distance much smaller than the instrumental resolution, and are thus invisible. Panels (a)–(c) are 1, 3, and 60 s after the quench, respectively. (d)–(f) The surfaces for the same times quenched to 847.3 °C, 1° beneath panels (a)–(c). Although the final surface structure is very similar, the growth mechanism is much different: It is difficult to resolve a time when isolated facets grow. (g)–(i) Surfaces quenched to 844.5 °C, 2.8 °C below the temperature of (d)–(f). Even only 1 s after the quench, there are no large regions of the surface which are unfaceted. The final length scale of the facets in panel (i) are much smaller than in panel (c). The complete lack of isolated nuclei suggests the analogy with spinodal decomposition. The field of view in all the panels is 4 μm.

large regions of the surface faceting in a coherent manner. (Although the final states of the surface 1 min after each quench are still similar.) There is no longer any time regime in which isolated facets grow. This change in kinetics is made even clearer in panels (g)–(i), which show a quench 2.8 °C beneath the temperature of panels (d)–(f). Rather than isolated nucleation and growth of linear facets, we instead see a simultaneous evolution of facets everywhere within the field of view. Notice the final width of the facets also changes as one would expect from the change in kinetics [from about 700 Å in Fig. 1(c) to about 300 Å in Fig. 1(i)]. Deeper quenches produce results virtually the same as those of panels (g)–(i).

We associate this dramatic change in kinetics with a change from nucleation and growth to spinodal decomposition. One distinctive characteristic of spinodal decomposition is the formation of a well-defined wavelength in the pattern of the phases [10]. (For example, the evolution of such a wavelength during the isothermal decomposition of an Al-Zn alloy has been observed using x-ray diffraction [15].) Figure 2 shows the time evolution of the absolute value of the Fourier transform of the sequence containing Fig. 1(g). A sharp peak, associated with a well-defined facet periodicity of about 600 Å, spontaneously develops within 1 s after the quench. (Such "spatial pattern formation" in the arrangements of facets has also been observed using high resolution electron diffraction by Falta, Imbihl, and Henzler [16] during the oxidation of CO on Pt.)

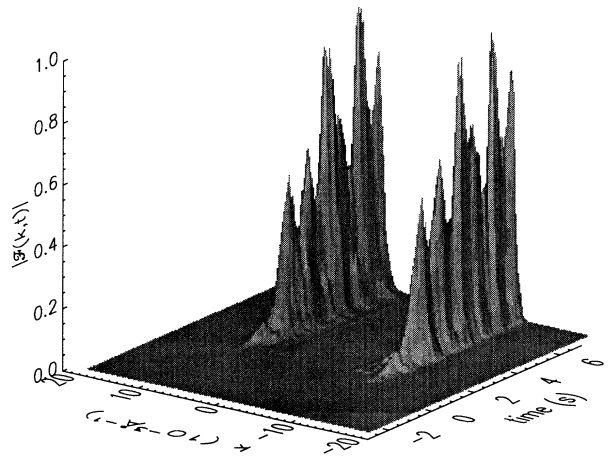

FIG. 2. The time dependence of the absolute value of the Fourier transform of the intensity of the sequence Fig. 1(g), showing that the facets evolve with well-defined periodicity, as is typical of spinodal decomposition.

Once the surface is completely covered by facets, i.e., no region of the surface is left unchanged from its high-temperature uniformly stepped state, there is no subsequent change in the number of facets over time scales on the order of tens of minutes. Evidently the time scale of "domain coarsening" associated with the merging of (111) facets is very long.

Before discussing the faceting kinetics, we review the thermodynamic driving force for the faceting. In the thermodynamic picture of the faceting of vicinal Si reviewed in Ref. [1], one identifies two free energy curves associated with the (1×1) and (7×7) phases. Each curve has a different dependence on the misorientation angle ϕ, and for small misorientations is expected to be of the form

$$f(\rho,T)=f^0(T)+\frac{\beta(T)}{h}\rho+g(T)\rho^3+\cdots, \qquad (1)$$

where $\rho=\tan(\phi)$ is the surface slope, $\beta(T)$ is the step free energy per unit length, h is the step height, and $g(T)$ is a measure of the step-step interactions. If the step energies are greater in the (7×7) phase than in the (1×1) phase, then the equilibrium surface is faceted over a range of misorientations, as shown in Fig. 3, because the combined free energy curves are not a convex function of the thermodynamic density ρ [17]. The surface slope of the (1×1) phase is then

$$\rho_0=(\Delta f^0/2g_{(1\times1)})^{1/3}, \qquad (2)$$

where Δf^0 is defined in Fig. 3. The temperature depen-

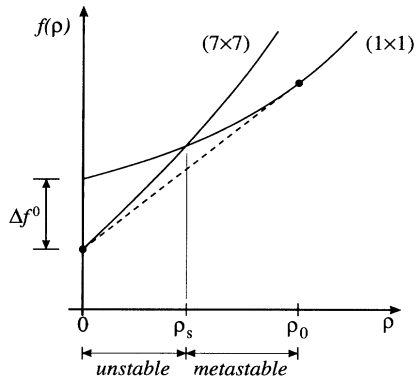

FIG. 3. The orientational dependence of the surface free energy believed to lead to the faceting of Fig. 1. Thermodynamics requires that the projected free energy be a convex function of $\rho = \tan(\phi)$. The free energies of the intersecting curves of the reconstructed and unreconstructed phases are not convex, leading to phase separation between the end points of the tie line (the dashed line).

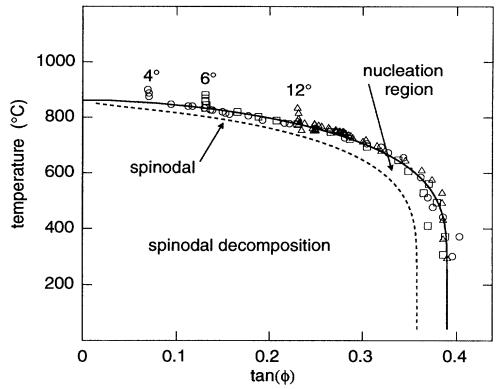

FIG. 4. The location of the spinodal (dashed line) on the temperature-orientation phase diagram of vicinal Si(111), as determined by the intersection of the free energy curves of the reconstructed and unreconstructed surfaces [Eq. (3)], using the estimates of step energies discussed in the text. The symbols are low-energy electron diffraction data from Ref. [2]. The solid line is a fit of the thermodynamic phase boundary to guide the eye.

dence of Δf^0 and $g_{(1\times1)}$ determines the shape of the temperature-orientation phase boundary through Eq. (2).

We now address the question of how one locates the spinodal from the thermodynamic scenario of Fig. 3. In the usual theory [10] one associates the spinodal with the points of inflection of the overall free energy curve. Because it has been shown experimentally that the interactions between the steps are repulsive in the (1×1) phase [18] and the (7×7) phase [19], both of the single-phase free energy curves in Fig. 3 are convex: Surfaces completely covered by (1×1) or (7×7) reconstruction are metastable with respect to faceting. (Thus the theory of Ref. [20] for the location of the spinodal for faceting does not appear to be directly applicable.) However, we now observe that the point where these two free energy curves cross will be associated with a change in the way the (7×7) phase can form. As indicated in Fig. 3, when the surface orientation angle is larger than that where the curves intersect, steps must rearrange locally to form large terraces before the surface can lower its free energy by forming the (7×7) reconstruction. Our observations for small quenches indicate such fluctuations in surface slope are rare. Thus the (1×1) surface is metastable with respect to (7×7) formation. On the other hand, at step densities below the point when the two curves cross, the formation of the (7×7) phase lowers the surface free energy without a requirement of step rearrangement: The surface is unstable with respect to formation of the (7×7) phase. We thus hypothesize that the point of intersection of the free energy curves corresponds to the location of the observed spinodal with nucleation for step densities greater than ρ_s and spinodal decomposition for densities less than ρ_s. This picture qualitatively accounts for the observation that nucleation rates increase near the spinodal: The barrier to the formation of the (7×7) reconstruction vanishes as the spinodal is approached.

We can be more quantitative about the predicted location of the spinodal. By equating the two free energy curves and using Eq. (2), the surface slope ρ_s at the spinodal line at any particular temperature can be written in terms of the slope ρ_0 at the phase boundary:

$$\frac{\beta_{(7\times7)}-\beta_{(1\times1)}}{h}\rho_s+(g_{(7\times7)}-g_{(1\times1)})\rho_s^3-2g_{(1\times1)}\rho_0^3=0. \quad (3)$$

Estimates of the step energies can be made from microscopic observations of terrace width distributions and step wandering [18,19]. As discussed at length in Ref. [21] assuming a plausible form for the kink Hamiltonians of the steps yields the estimates that, at 820 °C, $g_{(7\times7)} = 22\pm6$ meV/Å^2, $g_{(1\times1)} = 14\pm5$ meV/Å^2, and $\beta_{(7\times7)} - \beta_{(1\times1)} > 2$ meV/Å. Adjusting these values to minimize the size of the nucleation region (which, at 820 °C amounts to taking $g_{(7\times7)} = g_{(1\times1)} = 19$ meV/Å^2, and $\beta_{(7\times7)} - \beta_{(1\times1)} = 2$ meV/Å) and using the experimentally measured phase boundary $\rho_0(T)$ then yield the dashed curve in Fig. 4. For the 4° surface, the predicted spinodal lies 20 °C beneath the phase boundary, compared with the 9 °C we observe experimentally. Thus, our ideas about the step energetics of vicinal Si can correctly account for the order of magnitude of the distance of the spinodal beneath the phase boundary.

There are two additional pieces of information which also suggest the existence of a spinodal line of the form shown in Fig. 4: (1) We did not see a nucleation region on the 0.8° misoriented surface, suggesting the spinodal is very close to the phase buondary for this misorientation, as expected for small misorientations on the basis of Fig. 4. (If the nucleation regime exists, it presumably must be smaller than the 1 °C temperature stability of our sample.) (2) Hibino *et al.* [22] report a nucleation regime on a 10° misoriented surface of at least 25 °C,

which is much larger than the 9 °C we observe on the 4° surface.

As it stands, this theory only explains why there should be a sudden change in the kinetics of the formation of the (7×7) reconstruction. It does not explain why *faceting* should occur along with the formation of the (7×7). For example, if the steps at high temperature were arranged uniformly, one might expect that for $\rho < \rho_s$ (see Fig. 3) the (7×7) would form on all terraces simultaneously, leading to a uniformly stepped and metastable (7×7) reconstructed surface, which is not observed for this misorientation (but is for very small misorientations [23]).

To explain why faceting does occur when the formation of the (7×7) is not hindered by the presence of steps, we have performed simulations of faceting based on the thermodynamic picture of Fig. 3. The details of this work will be reported elsewhere [24]. However, the major conclusion of the simulations is that the surfaces are naturally unstable with respect to spatial *variations* in the step density or concentration of the (7×7) reconstruction. As an example, consider an initial modulation of the step density which is quenched beneath the spinodal. Given the thermodynamic picture of Fig. 3, it is natural to assume that the (7×7) reconstruction will grow most quickly on the wider terraces, leading to a variation in the concentration of the (7×7) reconstruction. This will lead to a variation in the chemical potential of Si atoms across the surface. This variation in chemical potential will drive a flux of atoms across the surface, making wide terraces even wider. The (7×7) reconstruction will in turn grow even more rapidly on these wider terraces causing an instability. The differential response of this instability with respect to perturbations of different wavelengths leads naturally to a wavelength selection [10,15], as we observe experimentally in Fig. 2. Linear stability analyses predict an exponential growth of the selected periodicity, also roughly consistent with our observations of Fig. 2. (Fits of the early time behavior to an exponential give a time constant on the order of 0.5 s.)

The explanation presented above is conceptually reasonable and consistent with estimates of step energetics. However, it is possible it is not a complete description because of the important role of surface stress at domain boundaries. In our previous report on nucleation of facets on vicinal Si(111) [3] we found that isolated facets [as seen in Figs. 1(a)–1(c)] had widths which after a short time did not grow. We proposed [8] that surface stress could be responsible for this width. Similarly, because of the remarkable fact that the bulk elastic relaxations associated with phase boundaries increase logarithmically with the distances between phase boundaries, periodic arrays of facets can be energetically preferred over infinitely large facets [25], providing an alternative explanation to our observations of a periodicity in Fig. 2. This effect could be important in quantitative theories of the location of the spinodal because by favoring the formation of domain boundaries between (1×1) and (7×7) reconstructions, elastic relaxation could change the temperature when isolated terraces become susceptible to the formation of the (7×7) reconstruction [20].

In summary, we have shown that the kinetics of the faceting of vicinal Si(111) changes dramatically over a very narrow temperature range. The change is from nucleation and growth to a regime analogous to spinodal decomposition observed in other phase separating systems [10,11,15]. We propose that this change is related to whether the (1×1) phase is metastable on terraces of width equal to the uniform high-temperature value.

This work was supported by the NSF under Grant No. DMR91-03031, by the Laboratory for Physical Sciences, and by the Volkswagen Foundation.

[1] E. D. Williams and N. C. Bartelt, Science **251**, 393 (1991).
[2] R. J. Phaneuf, E. D. Williams, and N. C. Bartelt, Phys. Rev. B **38**, 1984 (1988).
[3] R. J. Phaneuf *et al.*, Phys. Rev. Lett. **67**, 2986 (1991).
[4] T. E. Madey, K.-J. Song, and C.-Z. Dong, Surf. Sci. **247**, 175 (1991).
[5] J. C. Heyraud, J. J. Metois, and J. M. Bermond, J. Cryst. Growth **98**, 355 (1989).
[6] M. Flytzani-Stephanopoulos and L. D. Schmidt, Prog. Surf. Sci. **9**, 83 (1979).
[7] W. W. Mullins, Philos. Mag. **6**, 1313 (1961).
[8] E. D. Williams *et al.*, Mater. Res. Soc. Symp. Proc. **238**, 219 (1992).
[9] K. Binder, in *Materials Science and Technology: Phase Transformations in Materials,* edited by P. Haasen (VCH, Weinheim, 1990), Vol. 5, p. 405.
[10] J. W. Cahn, Trans. Met. Soc. AIME **242**, 167 (1968).
[11] K. Oki, H. Sagana, and T. Eguchi, J. Phys. (Paris), Colloq. **38**, C7-414 (1977).
[12] A. J. W. Moore, in *Metal Surfaces,* edited by W. D. Robertson and N. A. Gjostein (American Society for Metals, Metals Park, OH, 1962), p. 155.
[13] E. Bauer *et al.*, Ultramicroscopy **31**, 49 (1989).
[14] L. H. Veneklasen, Ultramicroscopy **36**, 76 (1991).
[15] K. B. Rundman and J. E. Hilliard, Acta Metall. **15**, 1025 (1966).
[16] J. Falta, R. Imbihl, and M. Henzler, Phys. Rev. Lett. **64**, 1409 (1990).
[17] P. Nozières, in *Solids Far From Equilibrium,* edited by C. Godrèche (Cambridge Univ. Press, Cambridge, 1991), p. 1.
[18] C. Alfonso *et al.*, Surf. Sci. **262**, 371 (1992).
[19] X.-S. Wang *et al.*, Phys. Rev. Lett. **65**, 2430 (1990).
[20] J. Stewart and N. Goldenfeld, Phys. Rev. A **46**, 6505 (1992).
[21] E. D. Williams *et al.*, Surf. Sci. (to be published).
[22] H. Hibino *et al.*, Phys. Rev. B **47**, 13027 (1993).
[23] W. Telieps *et al.*, Ber. Bunsen-Ges. Phys. Chem. **90**, 187 (1986).
[24] N. C. Bartelt (to be published).
[25] V. I. Marchenko, Zh. Eksp. Teor. Fiz. **81**, 1141 (1981) [Sov. Phys. JETP **54**, 605 (1981)].

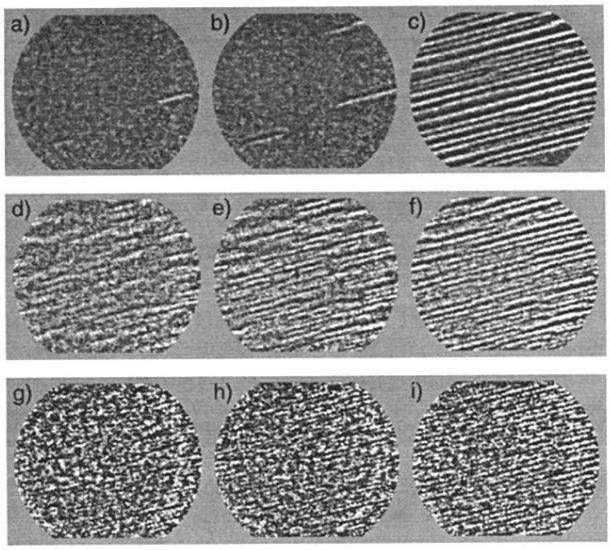

FIG. 1. (a)–(c) A sequence of LEEM images of vicinal Si quenched to 848.3 °C showing nucleation and growth. Initially the surface contains a uniform array of steps which are separated by a distance much smaller than the instrumental resolution, and are thus invisible. Panels (a)–(c) are 1, 3, and 60 s after the quench, respectively. (d)–(f) The surfaces for the same times quenched to 847.3 °C, 1° beneath panels (a)–(c). Although the final surface structure is very similar, the growth mechanism is much different: It is difficult to resolve a time when isolated facets grow. (g)–(i) Surfaces quenched to 844.5 °C, 2.8 °C below the temperature of (d)–(f). Even only 1 s after the quench, there are no large regions of the surface which are unfaceted. The final length scale of the facets in panel (i) are much smaller than in panel (c). The complete lack of isolated nuclei suggests the analogy with spinodal decomposition. The field of view in all the panels is 4 μm.